

Zhijun Lin^a, Yanchun Zhou^a, Meishuan Li^a, Jingyang Wang^{a,b}^aHigh-Performance Ceramic Division, Shenyang National Laboratory for Materials Science, Institute of Metal Research, Chinese Academy of Sciences, P. R. China^bInternational Centre for Materials Physics, Institute of Metal Research, Chinese Academy of Sciences, P. R. China

In-situ hot pressing/solid-liquid reaction synthesis of bulk Cr₂AlC

Single-phase bulk Cr₂AlC, a non-Ti-containing carbide with superior expected properties, was successfully fabricated by in-situ hot pressing/solid-liquid reaction process. The reaction process was investigated using differential scanning calorimetry. The products were characterized using X-ray diffraction and scanning electron microscopy. Four distinguished stages of the reactions from Cr, Al, and C elemental powders were discussed. The obtained X-ray diffraction data are in good agreement with calculated ones and those from JCPDS card No. 29-0017. A new set of X-ray diffraction data comprising reflections, 2θ , and intensities of Cr₂AlC is presented. Lattice parameters obtained by Rietveld XRD refinement of Cr₂AlC are $a = 2.858 \text{ \AA}$ and $c = 12.818 \text{ \AA}$, respectively. The measured Vickers hardness of the as-synthesized Cr₂AlC is $5.5 \pm 0.4 \text{ GPa}$, which is twice that of Ti₂AlC. Cr₂AlC displays excellent oxidation resistance. The parabolic rate constant of Cr₂AlC was decreased by 3–4 orders of magnitude compared with those of Ti₃SiC₂ at 1200 °C.

Keywords: Cr₂AlC; Solid-liquid reaction; XRD; Hardness; Oxidation

1. Introduction

The M_{n+1}AX_n phases, where M is an early transition metal, A is an A-group element (mostly IIIA and IVA) and X is either C and/or N, possess a unique combination of the merits of both metals and ceramics [1]. These merits include low density, high modulus, good thermal and electrical conductivity, excellent thermal shock and high-temperature-oxidation resistance, damage tolerance and easy machinability. The combination of these remarkable properties makes M_{n+1}AX_n phases highly promising candidates for diverse applications. Therefore, this family has received considerable attentions and has been extensively studied [1–23].

However, one drawback of most of the M_{n+1}AX_n phases is low hardness. For example, the Vickers hardness values of Ti₃SiC₂ [2], Ti₃AlC₂ [3], and Ti₂AlC [4] are 4.0 GPa, 2.5 GPa, and 2.8 GPa, respectively. Accordingly, several attempts have been made to increase the hardness of M_{n+1}AX_n phases by incorporating SiC, Al₂O₃, and TiC into Ti₃SiC₂ [5–7] or Ti₃AlC₂ [8]. The other drawback is that Ti-containing ternary carbides fail to form dense and protective oxide scales at intermediate temperatures (400–

650 °C) [9–11]. Thus, we aim to search for non-Ti containing compounds with better mechanical properties and corrosion resistance.

Recent theoretical works by Wang and Zhou [12], Sun et al. [13, 14], Schneider et al. [15], and Lofland et al. [16] demonstrate that Cr₂AlC possesses high elastic stiffness. According to Wang and Zhou [12], the theoretical shear modulus C_{44} , a factor that holds a direct relationship with hardness, was relatively high for Cr₂AlC in the (M_xM'_{2-x})AlC (M and M' = Ti, V, and Cr) system. As a result, relatively high intrinsic hardness might be achievable for Cr₂AlC. Furthermore, stoichiometric Cr₂AlC involves 72.7 wt.% of Cr and 18.9 wt.% Al. It is expected that protective α -Al₂O₃ and α -Cr₂O₃ films will form during oxidation of Cr₂AlC at high temperatures. These films will impart good corrosion resistance. Therefore, we anticipated specific outcomes: first, Cr₂AlC will be a relatively hard ternary carbide; second, it will exhibit good oxidation and corrosion resistance.

Despite these salient expected properties, only a few experimental works have been carried out on Cr₂AlC [15, 17, 18]. Jeitschko et al. [17] discovered Cr₂AlC and obtained its lattice parameters in the 1960s. It was determined that Cr₂AlC has the space group of P6₃/mmc with lattice parameters of $a = 2.86_0 \text{ \AA}$ and $c = 12.8_2 \text{ \AA}$. The 4 Cr atoms are in the Wyckoff positions of 4f, 2 Al atoms in 2d, and 2 C atoms in 2a. Schuster et al. [18] investigated the phase relationships in the ternary M₂AlC (M = Ti, V, and Cr) systems and confirmed the existence of M₂AlC, as well as the excellent miscibility of solid-solution series on M sites. Very recently, Schneider et al. [15] fabricated Cr₂AlC film by magnetron sputtering and obtained the structural parameters. To date, the reaction mechanism for the synthesis of bulk Cr₂AlC has not been reported. Since Cr₂AlC possesses attractive properties, we were motivated to synthesize bulk Cr₂AlC.

We developed an in-situ hot pressing/solid-liquid reaction method in previous work. Ti₃SiC₂ [19], Ti₃AlC₂ [20], and Ti₂AlC [4] were successfully fabricated by using this method. The prominent advantages of solid-liquid reaction are: energy cost effectiveness, short reaction time, and relatively low pressure requirement. Solid-liquid reaction is comparable with other alternative methods. For example, Tzenov and Barsoum [21] synthesized Ti₃AlC₂ by HIP at 1400 °C with 70 MPa pressure applied in 4 hours; Wang and Zhou [20] fabricated Ti₃AlC₂ using solid-liquid reaction at 1500 °C and 1200 °C with 25 MPa pressure applied for 5 min and 20 min, respectively. It is obvious that short reac-

tion time and lower applied pressure will result in energy cost effectiveness. In this paper, we report the reaction mechanism of Cr_2AlC synthesized by in-situ hot pressing/solid-liquid reaction process from Cr, Al, and C elemental powders. The term "solid-liquid reaction" for Cr_2AlC reflects the facts that Al melts at 660°C , and the eutectic reactions at 850°C and 1050°C produce liquid phases.

2. Experimental procedure

Commercially available elemental powders of Cr (99%, 200 mesh), Al (99.5%, 300 mesh), and graphite (99%, 200 mesh) were selected as initial materials. The molar ratio of Cr:Al:C was 2:1.05:1. Excess aluminum powder was added to compensate for the loss of Al during the heating process. To investigate the reaction mechanism, differential scanning calorimetry (DSC) was carried out in Ar atmosphere using a Setsys 16/18 thermal-analysis system (SETARAM, France). The powder mixtures of Cr, Al, and graphite were held in an alumina crucible and heated at a rate of $10^\circ\text{C}/\text{min}$ to 1400°C . Prior to fabricating bulk sample, the shrinkage behavior was also studied by loading compacted raw materials. The specimen with a diameter of 25 mm and a height of 8 mm, compacted in a graphite mold, was heated at a rate of $10^\circ\text{C}/\text{min}$. The applied load was 10 MPa during the entire deformation process. The compressive strain was defined as $-\Delta L/L_0$, where ΔL and L_0 represent, respectively, the shrinkage of sample height and the original height of the compacted specimen. During heating, a computer recorded the deformation of the sample continuously with an accuracy of $\pm 2\%$.

The bulk sample was prepared according to the following procedures. The mixed elemental powders were milled for 10 h in a polyurethane mill, using stainless-steel balls coated with a layer of polyurethane as the mixing media. The milled powders were sieved and compacted uniaxially in a graphite mold. The mold was 50 mm in diameter, 80 mm in height, and pre-sprayed with a BN layer. The compacted mixture was heated to 1400°C with a 60-min hold at an applied pressure of 5 MPa. Subsequently, it was annealed at 1350°C for 30 min, at which the applied pressure was increased to 30 MPa. The sintering process was conducted in a flowing Ar atmosphere at a heating rate of $15^\circ\text{C}/\text{min}$. The surface layer of the sample was machined off to remove the contaminants prior to characterization.

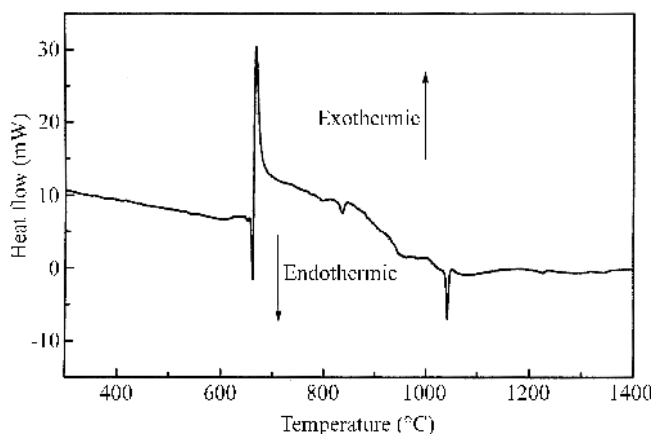


Fig. 1. DSC curve obtained with Cr, Al, C mixtures at a heating rate of $10^\circ\text{C}/\text{min}$ in Ar up to 1400°C .

Powders drilled from the samples were used for XRD analysis. The XRD data were collected by a step-scanning diffractometer with $\text{Cu-K}\alpha$ radiation (Rigaku D/max-2400, Japan). The data used to carry out a refinement had an accuracy better than 0.02° . The refinement was accomplished using the Rietveld method [24, 25] (a DBWS code in Cerius² computational program for material research, Molecular Simulation Inc., USA). The complete intensity profile of the powder diffraction pattern was refined by a non-linear least-square fitting of the Cr_2AlC structural model. The microstructure of the samples was studied by an S-360 scanning electron microscopy (Cambridge Instruments Ltd., UK) equipped with an energy-dispersive X-ray spectrometry (EDS) system.

The density of the specimen was determined by the Archimedes method. The Vickers hardness was tested at a load from 1 N to 10 N with the dwell time of 15 seconds. The surfaces of the specimen for the hardness test were polished to a $\sim 1\ \mu\text{m}$ diamond finish. For the oxidation study, specimen with dimensions of $3 \times 4 \times 15\ \text{mm}^3$ was cut by electrical-discharge machining method. The sample was ground down to 1000 grit SiC paper, polished using diamond paste, chamfered, and degreased in acetone. The sample was suspended with a Pt wire in a Setsys 16/18 thermogravimetric-analysis system (SETARAM, France). The weight gain was recorded continuously as a function of time at 1200°C in air.

3. Results

3.1. Reactions during heating

Figure 1 illustrates the DSC curve obtained by heating the mixed powders of Cr, Al, and graphite up to 1400°C at a heating rate of $10^\circ\text{C}/\text{min}$. Four distinguished peaks can be seen in the DSC curve. Figure 2 presents the XRD profiles for initial powder mixtures and those after holding at temperatures corresponding to the peaks in DSC curve for 20 minutes. In Fig. 1, a pronounced endothermic peak at the initial stage near 660°C corresponds to the melting of aluminum. Subsequently, a sharp exothermic peak is observed. XRD analysis suggests that this thermal explosion can be related to the formation of $\text{Cr}_9\text{Al}_{17}$ (Fig. 2b). At 850°C , XRD analysis indicates that the main equilibrium phases are Al_8Cr_5 , Cr, and graphite. The reflections of AlCr_2 (110) and AlCr_2 (103) were also identified (Fig. 2c). Based on XRD results, the endothermic peak near 850°C of the DSC curve originates from the eutectic reaction between AlCr_2 , Al_8Cr_5 , and Cr [26]. As can be seen in Fig. 2d, the desired Cr_2AlC forms at 1050°C .

Figure 3 shows the back-scattered electron images of the samples annealed at 700°C , 850°C , and 1050°C . Enlarged view of Fig. 3c is also shown in Fig. 3d for clarification. EDS analyses reveal that the dark regions contain mostly unreacted graphite, while the gray regions are mainly composed of Cr and Al, and the white regions comprise Cr. It can be seen in Fig. 3 that the microstructure of the samples is homogeneous. As the temperature increases, the relative amounts of Cr and graphite decrease while that of Cr-Al intermetallics increases. It is interesting to note that the gray regions seem to have closed connection with each other.

Figure 4 shows the compressive strain versus sintering temperature. Obvious shrinkage commences at approxi-

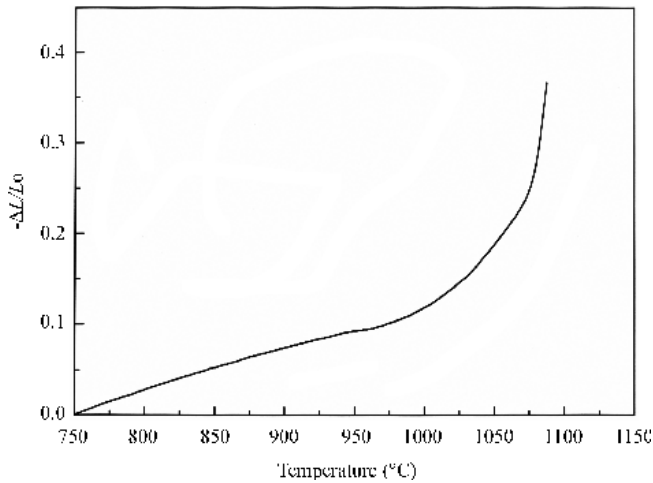
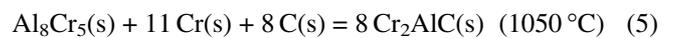
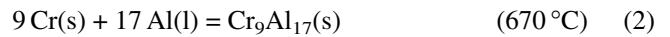


Fig. 4. Compressive strain of compacted raw materials versus temperature.

process as follows. Firstly, aluminum melts at about 660 °C. Subsequently, liquid Al reacts with Cr and produces significant amount of Cr₉Al₁₇ at about 670 °C. In the vicinity of 850 °C, Cr reacts with Cr₉Al₁₇ to produce AlCr₂ and Al₈Cr₅. Finally, Cr₂AlC forms through the reactions of Cr, graphite, AlCr₂, and Al₈Cr₅. The minor endothermic peak of the DSC curve in the vicinity of 850 °C arises from the eutectic reaction among AlCr₂, Al₈Cr₅, and Cr [26]. As can be seen in the DSC curve and Fig. 2d, another endothermic peak appears near 1050 °C with the increments of AlCr₂ and Cr₂AlC. Consequently, we assume that the increments of AlCr₂ and Cr₂AlC initiate another eutectic reaction. Thus, the liquid aspect of the “solid-liquid reaction” term reflects the two facts. First, liquid Al triggers a thermal

explosion reaction. Then the liquid phases produced by the eutectic reactions accelerate the formation of Cr₂AlC and expedite densification.

It is interesting that Cr₂AlC is detected while no reflections of Al₄C₃ or Cr₃C₂ appear (Fig. 2c). This phenomenon is consistent with that reported by Schuster et al. [18]. They reported that the only ternary carbide is more stable than the binary carbides Cr₃C₂ and Al₄C₃ at 800 °C. Based on the DSC, XRD, and SEM analyses, the whole reaction process in the temperature range from R.T. to 1050 °C can be depicted with the following equations:



4.2. Microstructure evolution

In Fig. 3, the homogeneous microstructures during heating favor the formation of Cr₂AlC. This ensures the high purity of the final product. At 700 °C, the thermal explosion reaction triggered by the melting of aluminum produced significant amount of Cr–Al intermetallics. EDS analysis revealed that the gray regions in Fig. 3 are composed of Cr and Al. At 850 °C and 1050 °C, the most distinguished change is that the relative amounts of Cr and graphite decrease while that of Cr–Al intermetallics increases. The decrease of chromium is probably due to the formation of Cr–Al intermetallics. Consumption of graphite during the

Table 1. Calculated, experimental, and JCPD card No. 29–0017 data of reflections, 2θ , and intensities for Cr₂AlC.

Reflections (h k l)	$2\theta_{\text{Cal.}}$ (°)	$2\theta_{\text{obs.}}$ (°)	$2\theta_{\text{JCPDS.}}$ (°)	$I/I_0_{\text{Cal.}}$ (%)	$I/I_0_{\text{obs.}}$ (%)	$I/I_0_{\text{JCPDS.}}$ (%)
0 0 4	27.880	27.762	27.857	1.87	1.75	2
1 0 0	36.268	36.215	36.236	18.75	16.32	20
1 0 1	36.965	36.909	36.930	6.60	5.41	7
1 0 2	38.991	38.927		0.02	0.47	
1 0 3	42.186	42.109	42.132	100.00	100.00	100
0 0 6	42.367	42.216	42.256	18.72	25.88	19
1 0 4	46.355	46.263	46.280	3.59	4.11	3
1 0 5	51.325	51.216		0.93	1.91	
1 0 6	56.968	56.840	56.858	16.05	17.74	12
0 0 8	57.607	57.418		0.01	0.07	
1 0 7	63.205	63.057		1.79	1.92	
1 1 0	65.243	65.197	65.185	18.11	19.53	12
1 1 2	67.060	67.007		1.41	1.45	
1 0 8	70.002	69.832		0.28	0.53	
1 1 4	72.380	72.305		0.58	0.92	
0 0 10	74.064	73.828		0.42	0.64	
2 0 0	76.995	76.953		1.80	2.25	
1 0 9	77.370	77.174	77.175	13.67	21.89	8
2 0 1	77.421	77.377		0.48	0.55	
2 0 2	78.696	787.647		0.00	0.04	
2 0 3	80.808	80.750		12.25	14.33	
1 1 6	80.931	80.823	80.840	14.21	18.85	10
2 0 4	83.744	83.765		0.44	0.31	

formation of Cr₂AlC accounts for the decrease of its content according to reactions (5) and (6). The reason that the gray regions seem to have close connection with each other can be attributed to the liquid phases produced during reactions,

i. e., Al melts near 660 °C, and the eutectic reactions produce liquid phases at elevated temperatures. The liquid formation reduces the reaction time and lowers the pressure requirement.

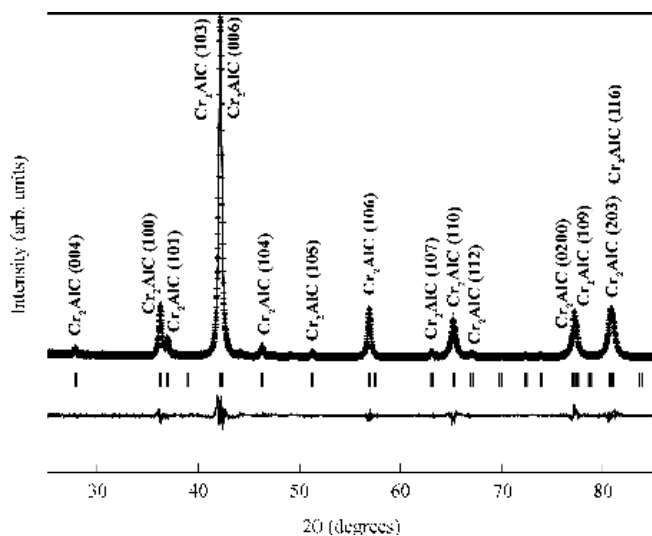


Fig. 5. Observed, calculated, and differential XRD profiles for Cr₂AlC.

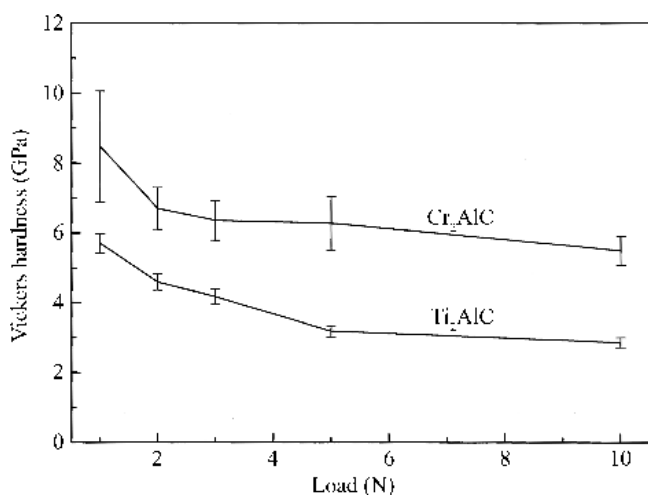


Fig. 6. Vickers hardness as a function of load of Cr₂AlC and Ti₂AlC.

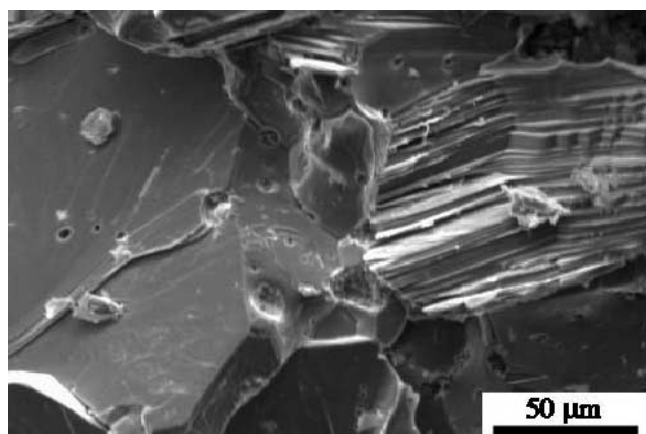


Fig. 7. SEM photograph of the as-synthesized Cr₂AlC.

4.3. Structural refinements, hardness, and oxidation kinetics

The experimental XRD pattern fits the calculated one well, which can be seen in Table 1 and Fig. 5. Only Cr₂AlC was detected. As it can be seen in Table 2, the refined lattice parameters agree well with those from Jeitschko et al. ($a = 2.86_0 \text{ \AA}$, $c = 12.8_2 \text{ \AA}$) [17], Schuster et al. ($a = 2.866 \text{ \AA}$, $c = 12.825 \text{ \AA}$) [18], and Schneider et al. ($a = 2.844 \text{ \AA}$, $c = 12.857 \text{ \AA}$) [15]. The deviation of the lattice parameters is less than 0.5 %. R-factors within 15 % are generally considered as a good refinement. The profiles (Fig. 5), as well as the refined lattice parameters and reliability factors confirm both the crystal structure of Cr₂AlC [15, 17] and the high purity of the as-synthesized specimen.

The high Vickers hardness values at low indentation loads are due to the elastic recovery that produced a smaller indent after indentation [2, 4]. The measured Vickers hardness value for Cr₂AlC is $5.5 \pm 0.4 \text{ GPa}$, which is approximately twice that of Ti₂AlC (2.8 GPa) [4]. This indicates

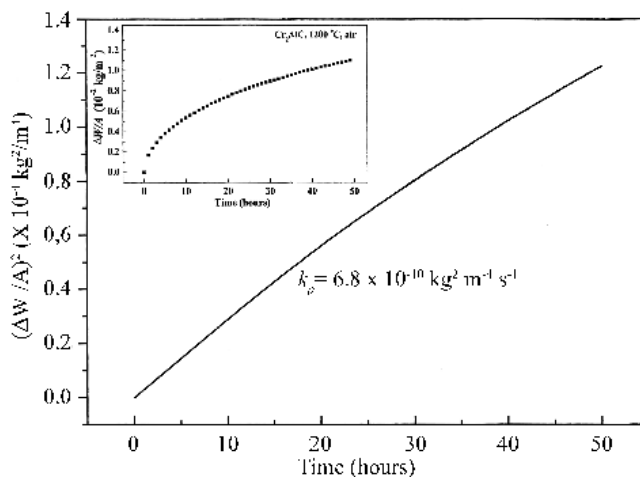
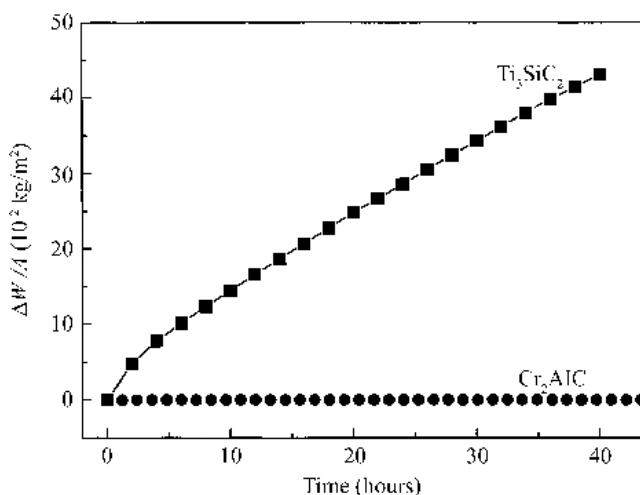


Fig. 8. (a) Mass gain per unit area versus time of Cr₂AlC and Ti₃SiC₂ at 1200 °C in air. (b) Square of weight gain per unit area as a function of time of Cr₂AlC at 1200 °C in air up to 50 hours. Inserted graph is the corresponding weight gain per unit area versus time of Cr₂AlC.

Table 2 Comparison of lattice parameters of Cr₂AlC obtained by Rietveld refinement and those from previous works

Lattice parameters		Reference
<i>a</i> (Å)	<i>c</i> (Å)	
2.858	12.818	Present work
2.86 ₀	12.8 ₂	
2.866	12.825	
2.844	12.857	

that Cr₂AlC is a relatively hard ternary carbide. The measured hardness values confirm the correctness of our previous prediction [12] based on first-principle calculations.

The parabolic rate constant, k_p , is $6.8 \times 10^{-10} \text{ kg}^2 \text{ m}^{-4} \text{ s}^{-1}$ for Cr₂AlC at 1200 °C. Compared with those of Ti₃SiC₂ ($6.58 \times 10^{-7} \text{ kg}^2 \text{ m}^{-4} \text{ s}^{-1}$ and $1.92 \times 10^{-6} \text{ kg}^2 \text{ m}^{-4} \text{ s}^{-1}$) [23], k_p decreased by 3–4 orders of magnitude. The low rate constant suggested that Cr₂AlC demonstrates excellent oxidation resistance.

5. Conclusions

Single-phase bulk Cr₂AlC was successfully fabricated through in-situ hot pressing/solid liquid reaction process using Cr, Al, and graphite powders as initial materials. The main intermediate phases were Cr₉Al₁₇, Al₈Cr₅, and AlCr₂ in the 700–1050 °C ranges for Cr₂AlC synthesized from elemental powders. The present process confirms the advantages of solid liquid reaction on fabricating bulk Cr₂AlC as short reaction time, energy cost effectiveness, and relatively low pressure requirement. Rietveld XRD refinement resulted in following lattice parameters for Cr₂AlC: $a = 2.858 \text{ Å}$ and $c = 12.818 \text{ Å}$. They are in excellent agreement with previously reported data. The deviation of lattice parameters is less than 0.5%. A new complete set of XRD reflections, 2θ , and intensities for Cr₂AlC is presented. The measured Vickers hardness of Cr₂AlC is $5.5 \pm 0.4 \text{ GPa}$, which is about twice that of Ti₂AlC. Excellent high-temperature oxidation resistance endows Cr₂AlC an ideally hard ternary carbide for high-temperature applications.

This work was supported by the National Outstanding Young Scientist Foundation for Y. C. Zhou under Grant No. 59925208, Natural Sciences Foundation of China under Grant No. 50232040, No. 50072034, '863' project, and High-tech Bureau of the Chinese Academy of Sciences. The authors thank Ms Jeanine McCartan from Chicago for technically reviewing this manuscript.

References

- [1] M.W. Barsoum: Prog. Solid State Chem. 28 (2000) 201.
- [2] T. El-Raghy, A. Zavaliangos, M.W. Barsoum, S.R. Kalidindi: J. Am. Ceram. Soc. 80 (1997) 513.
- [3] X.H. Wang, Y.C. Zhou: Acta. Mater. 50 (2002) 3141.
- [4] X.H. Wang, Y.C. Zhou: Z Metallkd. 93 (2002) 66.
- [5] X.H. Tong, T. Okano, T. Iseki, T. Yano: J. Mater. Sci. 30 (1995) 3087.
- [6] Y.M. Luo, S.Q. Li, J. Chen, R.G. Wang, J.Q. Li, W. Pan: J. Am. Ceram. Soc. 85(2002) 3099.
- [7] L.H. Ho-Duc, T. El-Raghy, M.W. Barsoum: J. Alloys Comp. 350 (2003) 303.
- [8] J.X. Chen, Y.C. Zhou: Scripta Mater. 50 (2004) 897.
- [9] C. Racault, F. Langlais, R. Naslain: J. Mater. Sci. 29 (1994) 3384.
- [10] X.H. Wang, Y.C. Zhou: Mater. Res. Innovat. 7 (2003) 381.
- [11] X.H. Wang, Y.C. Zhou: J. Mater. Res. 17(2002) 2974.
- [12] J.Y. Wang, Y.C. Zhou: J. Phys. Condens. Matter 16 (2004) 2819.
- [13] Z.M. Sun, R. Ahuja, J.M. Schneider: Phys. Rev. B 68 (2003) 224112.
- [14] Z.M. Sun, R. Ahuja, S. Li, J.M. Schneider: Appl. Phys. Lett. 83 (2004) 899.
- [15] J.M. Schneider, Z.M. Sun, R. Mertens, F. Uestel, R. Ahuja: Solid State Commun. 130 (2004) 445.
- [16] S.E. Lofland, J.D. Hettinger, K. Harrell, P. Finkel, S. Gupta, M.W. Barsoum, G. Hug: Appl. Phys. Lett. 84 (2004) 508.
- [17] W. Jeitschko, H. Nowotny, F. Benesovsky: Monatsh. Chem. 94 (1963) 672.
- [18] J.C. Schuster, H. Nowotny, C. Vaccaro: J. Solid State Chem. 32 (1980) 213.
- [19] Y.C. Zhou, Z.M. Sun, S.Q. Chen, Y. Zhang: Mater. Res. Innovat. 2 (1998) 142.
- [20] X.H. Wang, Y.C. Zhou: J. Mater. Chem. 12 (2002) 455.
- [21] N.V. Tzenov, M.W. Barsoum: J. Am. Ceram. Soc. 84 (2000) 825.
- [22] Z.M. Sun, Y.C. Zhou, M.S. Li: Corros. Sci. 43 (2001) 1095.
- [23] M.W. Barsoum, T. El-Raghy, L. Ogbuji: J. Electrochem. Soc. 144 (1997) 2508.
- [24] R.A. Young: The Rietveld Method, Oxford University Press (1993).
- [25] D.B. Wiles, R.A. Young: J. Appl. Crystallogr. 14 (1981) 149.
- [26] J.L. Murray: Binary Alloy Phase Diagrams, ASM International Materials Park, Ohio (1990) 138.

(Received July 15, 2004; accepted October 22, 2004)

Correspondence address

Dr. Yanchun Zhou
 Professor and Director of High-performance Ceramic Division
 Shenyang National Laboratory for Materials Science
 Institute of Metal Research, Chinese Academy of Sciences
 72 Wenhua Road, Shenyang, 110016, P. R. China
 Tel.: +86 24 2397 1765
 Fax: +86 24 2389 1320
 E-mail: yczhou@imr.ac.cn